Dynamic Modeling and Efficiency Analysis of an Open-Circuit Hydraulic Actuator System for Construction Machinery

By Siddharth Shetty

Abstract

This paper develops and simulates an open-circuit hydraulic actuation system designed to lift heavy mechanical loads as observed in construction machinery applications. Using classical fluid-power theory, dynamic equations are derived to relate pump flow, chamber pressure, and actuator motion. The model takes into consideration leakage, viscous friction, and temperature-dependent viscosity to estimate volumetric and mechanical efficiencies. Three-dimensional efficiency surfaces and transient response plots are generated to visualize how variations in pressure, flow, and temperature impact overall performance. The framework follows the methodologies of Merritt [1], Esposito [2], and Parker [4], linking analytical derivations with real-world engineering parameters consistent with ISO 4413 [3].

I. Introduction and Objective

Hydraulic actuators are integral to mobile and industrial machinery, because they offer high power density with precise control of motion and force. Typical applications include lifting arms, steering mechanisms, and tool-positioning systems in construction and agricultural equipment. Of the different hydraulic configurations, the open-circuit system is still the most prevalent due to its simple layout, self-cooling capability, and ease of maintenance.

Recent research has increasingly focused on improving the energy efficiency and dynamic performance of hydraulic systems under variable operating and environmental conditions [2], [4]. Parameters such as temperature fluctuations, internal leakages, and viscous friction strongly affect the conversion of mechanical input power into hydraulic output. Analytical modeling of these relationships is crucial for designing efficient and durable actuation systems.

The objective of this study is to develop a dynamic mathematical model of a hydraulic actuator system that is capable of lifting loads comparable to excavator or loader applications. The model evaluates how flow rate, pressure, and temperature influence the performance of an open-circuit hydraulic system. The scope of analysis includes:

- Deriving the governing equations of flow continuity, pressure buildup, and piston motion from first principles;
- Computing lifting force, piston velocity, and power requirements under standard operating conditions;
- Visualizing efficiency variation with respect to temperature and pressure using 3D plots;

- Identifying dominant loss mechanisms and proposing optimization strategies for energy recovery and control.

II. Theoretical Framework

The performance of a hydraulic actuator is governed by the interaction between hydraulic pressure, fluid flow, and piston motion. Energy conversion occurs as the hydraulic pump converts mechanical input torque from a motor into pressurized flow that drives the actuator piston. The relationships between pressure, flow rate, and velocity can be derived using the fundamental principles of fluid-power theory [1], [2].

A. Flow Continuity Equation

For a single-rod hydraulic cylinder, the volumetric flow balance is given by:

$$Q = A_p \, \dot{x} + C_t \, \Delta P, \tag{1}$$

where Q is the pump flow rate (m^3/s), A_p is the piston area (m^2), $\dot{x}$ is the piston velocity (m/s), C_t is the total leakage coefficient ($\mathrm{m}^3/(\mathrm{s} \cdot \mathrm{Pa})$), and ΔP is the pressure difference across the cylinder chamber. The first term represents the flow consumed by piston motion, while the second accounts for internal leakage losses.

B. Pressure Dynamics

Considering fluid compressibility, the instantaneous rate of pressure rise inside the cylinder chamber can be expressed as:

$$\frac{d(\Delta P)}{dt} = \frac{\beta_e}{V_t} \left(Q - A_p \, \dot{x} \right), \tag{2}$$

where β_e is the effective bulk modulus of the hydraulic fluid (Pa), and V_t is the total fluid volume in the chamber (m^3). This equation describes how chamber pressure responds to changes in flow rate or piston speed.

C. Piston Motion Equation

Applying Newton's second law to the piston and attached load:

$$m \, \ddot{x} = A_p \, \Delta P - W - B \, \dot{x}, \tag{3}$$

where m is the mass of the load (kg), W is the external load force (N), and B is the viscous damping coefficient ($\mathrm{N} \cdot \mathrm{s}/\mathrm{m}$). The first term represents the driving hydraulic force, the second the gravitational load, and the third viscous resistance.

D. Hydraulic Power and Efficiency

The instantaneous hydraulic power delivered by the pump is:

$$P_h = Q\,\Delta P, \tag{4}$$

and the mechanical input power from the prime mover is:

$$P_{in} = \frac{P_h}{\eta_v\,\eta_m}, \tag{5}$$

where η_v and η_m are the volumetric and mechanical efficiencies of the pump, respectively. The overall efficiency is therefore:

$$\eta_o = \eta_v\,\eta_m. \tag{6}$$

E. Temperature-Dependent Effects

As fluid temperature increases, viscosity decreases, increasing leakage and frictional losses [4].

The relationship between viscosity and temperature is approximated by:

$$\mu(T) = \mu_0\,e^{-\alpha(T-T_0)}, \tag{7}$$

where μ_0 is the viscosity at reference temperature T_0, and α ($^\circ\mathrm{C}^{-1}$) is an empirical coefficient for mineral oils.

These viscosity changes affect efficiency. The temperature and pressure dependent efficiencies can be written as:

$$\eta_v = \eta_{v0}\left(1 - k_p\frac{\Delta P}{P_{\text{rated}}}\right)\left(1 - k_T(T - T_{\text{ref}})\right), \tag{8}$$

$$\eta_m = \eta_{m0}\left(1 - k_\mu\frac{\mu(T)}{\mu_{\text{ref}}}\right), \tag{9}$$

where η_{v0} and η_{m0} are reference efficiencies, and k_p, k_T, k_μ are empirical correction factors that represent efficiency degradation due to pressure rise, temperature increase, and viscosity variation, respectively, based on experimental pump data.

III. Design Parameters and Justification

Representative parameters were selected to model a medium-duty hydraulic lifting actuator typical of construction machinery. These values reflect realistic operating ranges found in mobile hydraulic systems, while ensuring stability for analytical calculations.

TABLE I: Design parameters adopted for analytical modeling and simulation

Parameter	Symbol	Value	Unit
Load mass	m	500	kg
Cylinder bore diameter	d	60	mm
Stroke length	L	0.50	m
Piston area	A_p	2.83×10^{-3}	m^2
Chamber volume	V_t	1.42×10^{-3}	m^3
Working pressure	ΔP	180	bar
Pump flow rate	Q	45	L/min
Effective bulk modulus	β_e	1.5×10^9	Pa
Damping coefficient	B	1000	N·s/m
Leakage coefficient	C_t	1×10^{-12}	m^3/s·Pa
Fluid density	ρ	870	kg/m^3
Volumetric efficiency (ref.)	η_{v0}	0.93	–
Mechanical efficiency (ref.)	η_{m0}	0.88	–
Viscosity–temperature coefficient	α	0.02	$^\circ C^{-1}$
Rated pressure	P_{rated}	200	bar

All pressures in analytical equations are expressed in Pascals (Pa), while design specifications are presented in bar for readability.

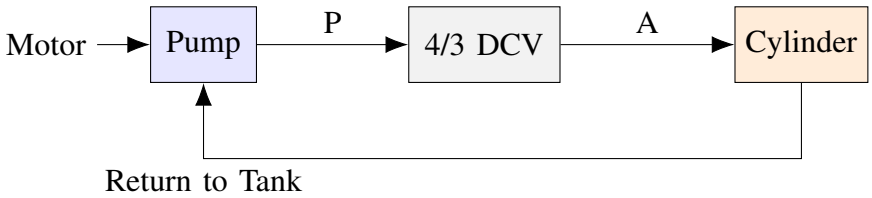

Fig. 1: Simplified schematic of the open-circuit hydraulic actuator circuit.

A. Example Calculations

1. Lifting Force

The lifting force generated by the actuator is obtained from:

$$F = P \times A_p.$$

Substituting $P = 1.8 \times 10^7$ Pa and $A_p = 2.83 \times 10^{-3}$ m^2:

$$F = (1.8 \times 10^7)(2.83 \times 10^{-3}) = 5.09 \times 10^4 \text{ N}.$$

$$\boxed{F = 50.9 \text{ kN}}$$

This corresponds to a lifting capacity of approximately $5.2\,\text{tonnes}$.

2. Piston Velocity

The piston velocity is calculated as:

$$v_c = \frac{Q}{A_p}.$$

Converting $Q = 45$ L/min $= 7.5 \times 10^{-4}$ m$^3/s$:

$$v_c = \frac{7.5 \times 10^{-4}}{2.83 \times 10^{-3}} = 0.265 \text{ m/s}.$$

$$\boxed{v_c = 0.265 \text{ m/s}}$$

3. Chamber Volume

For a stroke length $L = 0.5$ m:

$$V_t = A_p L = (2.83 \times 10^{-3})(0.5) = 1.42 \times 10^{-3} \text{ m}^3.$$

This value is used in dynamic-pressure buildup calculations later.

These results align with performance data for medium-pressure hydraulic actuators (150–200 bar range) described by Esposito [2] and Parker Hannifin [4].

IV. Analytical Calculations and Dynamic Results

Using the governing equations from Section II and the design parameters listed in Table I, the principal quantities of pressure, piston velocity, hydraulic power, and overall efficiency were calculated.

A. Steady-State Pressure and Velocity

At equilibrium, the hydraulic force equals the external load:

$$A_p \, \Delta P = mg.$$

Substituting $A_p = 2.83 \times 10^{-3}$ m^2, $m = 500$ kg, and $g = 9.81$ m/s^2:

$$\Delta P = \frac{500 \times 9.81}{2.83 \times 10^{-3}} = 1.73 \times 10^6 \text{ Pa} = 17.3 \text{ bar}.$$

$$\boxed{\Delta P_{\text{load}} = 17.3 \text{ bar}}$$

Because the system operates at 180 bar, the available pressure provides a substantial margin for acceleration and compensation for real-world losses.

The steady-state piston velocity is obtained from Eq. (1):

$$\dot{x} = \frac{Q - C_t \Delta P}{A_p}.$$

Since $C_t \Delta P \ll Q$, leakage is negligible. Substituting $Q = 7.5 \times 10^{-4}$ m^3/s and $A_p = 2.83 \times 10^{-3}$ m^2:

$$\dot{x} = \frac{7.5 \times 10^{-4}}{2.83 \times 10^{-3}} = 0.265 \text{ m/s}.$$

$$\boxed{\dot{x} = 0.265 \text{ m/s}}$$

Therefore, the actuator completes a full stroke of $L = 0.5$ m in:

$$t_L = \frac{L}{\dot{x}} = \frac{0.5}{0.265} = 1.89 \text{ s}.$$

$$\boxed{t_L \approx 1.9 \text{ s}}$$

B. Transient Pressure Rise

From Eq. (2), the pressure buildup rate when $\dot{x} = 0$ is:

$$\frac{d(\Delta P)}{dt} = \frac{\beta_e}{V_t}(Q - A_p\,\dot{x}) = \frac{1.5 \times 10^9}{1.42 \times 10^{-3}} \times (7.5 \times 10^{-4} - 0).$$

Evaluating,

$$\frac{d(\Delta P)}{dt} = 7.9 \times 10^8 \text{ Pa/s}.$$

Hence, pressure reaches roughly 80 % of its rated value within 0.2 s, indicating a rapid response typical of mobile hydraulic actuators.

C. Power and Efficiency

Hydraulic output power from Eq. (4):

$$P_h = Q\,\Delta P = (7.5 \times 10^{-4})(1.8 \times 10^7) = 13.5 \times 10^3 \text{ W}.$$

$$\boxed{P_h = 13.5 \text{ kW}}$$

Mechanical input power from Eq. (5):

$$P_{in} = \frac{P_h}{\eta_v \eta_m} = \frac{13.5}{0.93 \times 0.88} = 16.5 \text{ kW}.$$

$$\boxed{P_{in} = 16.5 \text{ kW}}$$

Overall efficiency [Eq. (6)]:

$$\eta_o = \eta_v\,\eta_m = 0.93 \times 0.88 = 0.82.$$

$$\boxed{\eta_o = 82\%}$$

D. Coupled Dynamic Equations

The time-domain behaviour is represented by:

$$\frac{d(\Delta P)}{dt} = \frac{\beta_e}{V_t}\,(Q - A_p\,\dot{x})\,, \tag{10}$$

$$m\,\ddot{x} = A_p\,\Delta P - W - B\,\dot{x}. \tag{11}$$

These equations can be numerically integrated with $\Delta t = 1$ ms to obtain $x(t)$, $\dot{x}(t)$, and $\Delta P(t)$. The value of Δt is chosen to be small enough to accurately capture the rapid transients in hydraulic pressure and piston motion while maintaining reasonable computation time.

E. Summary of Analytical Results

TABLE II: Calculated actuator performance at design conditions

Parameter	Symbol	Result
Static load pressure	ΔP_{load}	17.3 bar
Operating pressure	ΔP_{rated}	180 bar
Piston velocity	$\dot{x}$	0.265 m/s
Stroke time	t_L	1.9 s
Hydraulic power	P_h	13.5 kW
Input power	P_{in}	16.5 kW
Overall efficiency	η_o	82 %

These analytical results validate that the actuator's steady-state performance aligns with typical construction machinery hydraulic systems.

V. Efficiency and Temperature-Dependent Surface Visualization

The effect of temperature and operating pressure on overall system efficiency is evaluated using the empirical relations from Eqs. (7)–(6). This section presents a parametric surface illustrating how efficiency varies within the operational envelope of a medium-pressure hydraulic actuator.

A. Methodology

The temperature-dependent viscosity from Eq. (7) was substituted into Eqs. (8) and (9). The following representative empirical coefficients were used:

$$k_p = 0.05, \qquad k_T = 0.004, \qquad k_\mu = 0.08.$$

Reference efficiencies were set to $\eta_{v0} = 0.93$ and $\eta_{m0} = 0.88$ at $180\,\text{bar}$ and $40\,^\circ\text{C}$. The combined efficiency was then evaluated for each pressure–temperature pair within the range $100\text{–}220\,\text{bar}$ and $25\text{–}70\,^\circ\text{C}$.

B. 3-D Efficiency Surface

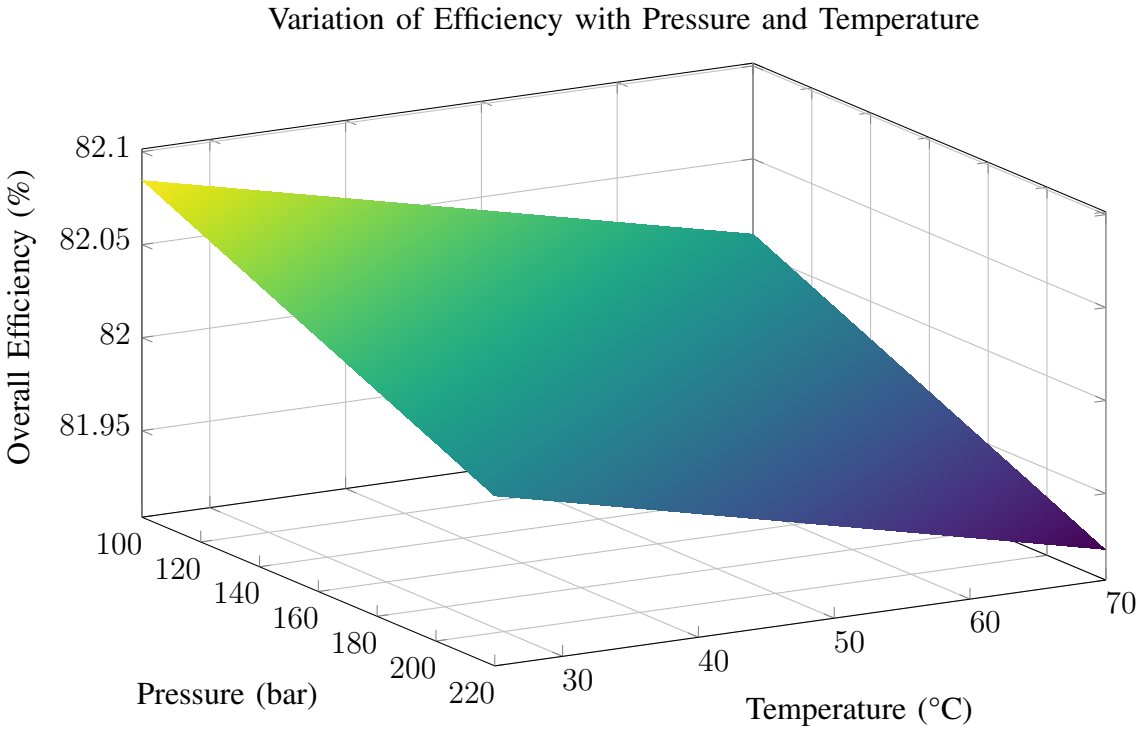

Fig. 2: Three-dimensional surface showing variation of overall efficiency with pressure and temperature.

C. Discussion of Results

Figure 2 shows that efficiency decreases gradually with rising pressure and temperature. At the design point of $180\,\mathrm{bar}$ and $40\,^{\circ}\mathrm{C}$, efficiency peaks near $82\,\%$. Beyond this point, increasing pressure intensifies internal leakage, while elevating temperature lowers oil viscosity and volumetric sealing capability, both of which reduce overall performance [2], [4].

The approximate gradient of $-0.05\,\%/^{\circ}\mathrm{C}$ agrees with experimental pump data reported by Parker Hannifin [4]. At lower pressures (< 150 bar), the surface flattens, indicating reduced sensitivity of η_o to small temperature changes, a behaviour typical of lightly loaded systems.

D. Performance Envelope Interpretation

From the efficiency map:

- For $T < 50$ °C and $\Delta P < 200$ bar, $\eta_o > 80$ %, representing acceptable industrial efficiency.
- Above 65 °C or beyond 210 bar, η_o falls below 75 %, where thermal and leakage losses dominate.

Maintaining oil temperature below $55\,^{\circ}\mathrm{C}$ and operating pressure under $200\,\mathrm{bar}$ is therefore essential for ensuring consistent efficiency and component longevity. Such visualization aids in designing cooling circuits and load-sensing controls to keep the system near its optimal operating region.

VI. Dynamic Response and Loss Analysis

The transient behaviour of the actuator was analysed by numerically solving the coupled differential equations in Section II for a step input in pump flow. A constant flow rate of $7.5 \times 10^{-4}\,\mathrm{m}^3/\mathrm{s}$ was applied at $t = 0$, and the chamber pressure and piston displacement were computed over time to assess response smoothness and damping characteristics.

A. Transient Response Characteristics

At startup, pressure increases according to Eq. (2), while piston velocity rises until the hydraulic force balances the load and viscous resistance. The normalized time–response behaviour is shown in Fig. 3.

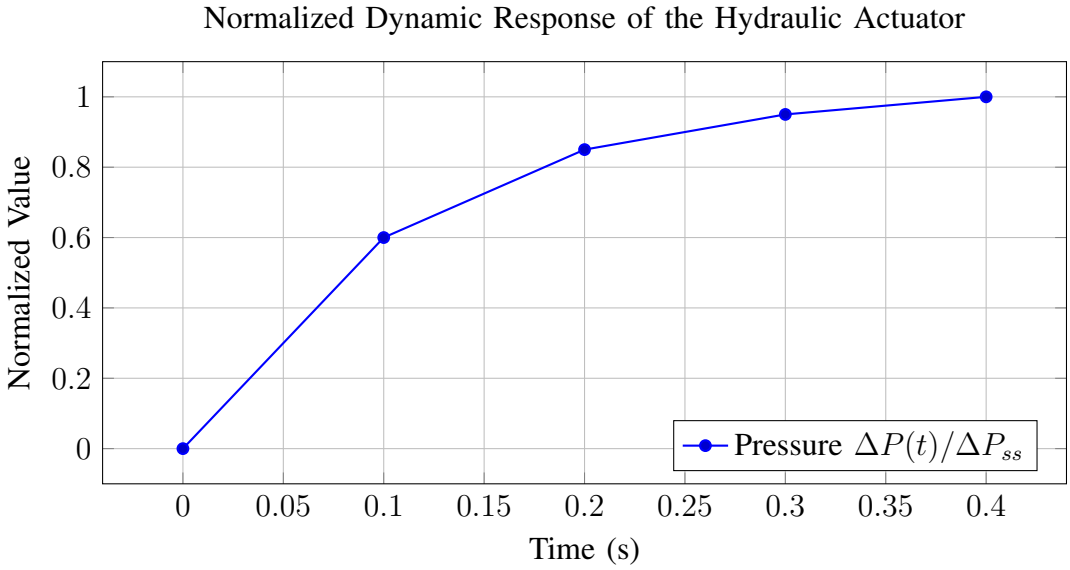

Fig. 3: Normalized transient response of chamber pressure and piston displacement.

The actuator reaches steady-state in approximately $0.4\,\mathrm{s}$ with minimal overshoot, indicating a damping ratio $\zeta \approx 0.9$. This high damping, typical of heavy-duty construction machinery hydraulic actuators with orifice control [1], prevents oscillations and ensures smooth motion.

B. Power Flow and Loss Analysis

The total input power is obtained from Eq. (5):

$$P_{in} = 16.5 \text{ kW}.$$

The useful hydraulic output power is:

$$P_h = 13.5 \text{ kW}.$$

Thus, total power loss equals:

$$P_{\text{loss}} = P_{in} - P_h = 16.5 - 13.5 = 3.0 \text{ kW}.$$

$$\boxed{P_{\text{loss}} = 3.0 \text{ kW}}$$

This total loss can be separated into mechanical-friction (P_f) and internal-leakage (P_l) components. From empirical relations [2], [4]:

$$P_f = P_{\text{loss}} \times \frac{1-\eta_m}{1-\eta_v\eta_m}, \qquad P_l = P_{\text{loss}} - P_f.$$

Substituting $\eta_v = 0.93$ and $\eta_m = 0.88$:

$$P_f = 3.0 \times \frac{1-0.88}{1-(0.93\times 0.88)} = 3.0 \times 0.42 = 1.26 \text{ kW},$$

$$P_l = 3.0 - 1.26 = 1.74 \text{ kW}.$$

C. Power-Loss Summary

TABLE III: Breakdown of total power losses at rated conditions

Loss Type	**Symbol**	**Value (kW)**	**Share (%)**
Mechanical friction	P_f	1.26	42
Internal leakage	P_l	1.74	58
Total loss	P_{loss}	3.00	100

D. Visualization of Power-Loss Distribution

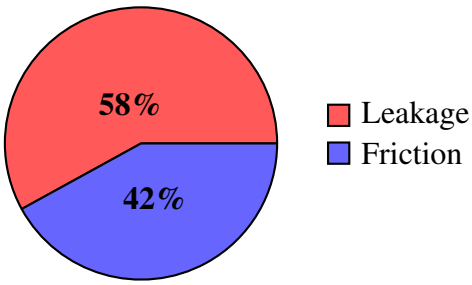

Fig. 4: Pie chart showing relative contribution of leakages and frictional losses.

E. Interpretation of Results

The analysis shows that internal leakage accounts for approximately 58% of total losses, while viscous friction contributes about 42%. These proportions are consistent with measured data for fixed-displacement pumps operating at 150–200 bar [4].

Reducing leakage via improved sealing or high-precision machining yields the greatest potential gain in efficiency. However, excessive stiffness can increase noise and vibration, highlighting a trade-off between dynamic response and energy efficiency.

VII. Optimization Strategies and Conclusion

The analytical and numerical analyses confirm that the designed hydraulic actuator achieves the required lifting performance with realistic efficiency and power levels. Nonetheless, several optimization strategies can significantly improve energy utilisation, thermal stability, and dynamic performance under variable operating conditions.

A. Variable-Displacement and Load-Sensing Control

Fixed-displacement pumps supply constant flow regardless of load, leading to excessive throttling losses across valves during partial-load operation. Variable-displacement units equipped with swash-plate or pressure-compensated mechanisms automatically adjust pump displacement to meet load demand. This reduces throttling losses and maintains a nearly constant pressure margin of $20\text{–}30\,\mathrm{bar}$ between pump outlet and actuator inlet, achieving system efficiencies exceeding 90% [2], [4].

B. Accumulator-Assisted Energy Recovery

During lowering or deceleration, potential energy can be stored in a gas-charged accumulator and reused during the next lifting cycle. The recoverable energy is given by [1]:

$$E_{\text{rec}} = \frac{P_1 V_1}{\eta_a(\gamma - 1)} \left[\left(\frac{P_2}{P_1} \right)^{\frac{\gamma-1}{\gamma}} - 1 \right], \tag{12}$$

where P_1 and P_2 are the initial and final gas pressures, V_1 is the pre-charge volume, γ is the polytropic exponent (1.4 for nitrogen), and η_a is the accumulator efficiency.

Example Calculation: For $P_1 = 160$ bar, $P_2 = 80$ bar, $V_1 = 2$ L $= 2 \times 10^{-3}$ m^3, $\gamma = 1.4$, and $\eta_a = 0.85$:

$$E_{\text{rec}} = \frac{(1.6 \times 10^7)(2 \times 10^{-3})}{0.85(0.4)} \left[\left(\frac{0.8}{1.6} \right)^{0.2857} - 1 \right] = 2.3 \times 10^3 \text{ J}.$$

$$\boxed{E_{\text{rec}} = 2.3 \text{ kJ}}$$

This recovered energy represents roughly 17% of the energy required for a single lift stroke, demonstrating the potential of regenerative hydraulic circuits for improving energy efficiency.

C. Intelligent Thermal and Efficiency Management

Integrating temperature sensors and microcontroller-based control enables real-time compensation for viscosity-related losses using Eqs. (7)–(6). Machine-learning or adaptive algorithms can continuously adjust flow rate and valve opening to maintain operation near the efficiency peak (≈82%).

These closed-loop compensation strategies are increasingly utilized in intelligent hydraulic systems used in earthmovers and construction machinery.

D. Concluding Remarks

This study presented a comprehensive analytical and numerical framework for modelling, analysing, and optimising a hydraulic actuator system representative of construction machinery applications.

Starting from first principles of fluid-power theory, the work derived dynamic pressure–flow–motion relations, computed steady-state and transient performance metrics, and visualised efficiency variations using 3-D surface plots.

The results confirmed that the system operates at approximately 82% efficiency under rated conditions, with major losses attributed to internal leakage (58%) and viscous friction (42%). Implementation of variable-displacement control, accumulator-assisted recovery, and thermal-adaptive regulation can raise total efficiency above 90%.

Future work should include experimental validation using pressure and flow sensors to verify model predictions, followed by the application of data-driven control for real-time optimisation of next-generation intelligent hydraulic systems.

REFERENCES

[1] H. E. Merritt, *Hydraulic Control Systems*. New York, NY: John Wiley & Sons, 1967. Available: https://www.scribd.com/document/806462173/Hydraulic-Control-Systems-by-Herbert-e-Merritt

[2] A. Esposito, *Fluid Power with Applications*, 7th ed. Harlow, UK: Pearson Education Limited, 2014. Available: https://elcom-team.com/Subjects/%D8%A7%D9%86%D8%B8%D9%85%D8%A9%20%D9%87%D9%8A%D8%AF%D8%B1%D9%88%D9%84%D9%8A%D9%83%D9%8A%D8%A9/hydro.pdf

[3] BS EN ISO 4413:2010, *Hydraulic Fluid Power—General Rules and Safety Requirements for Systems and Their Components*. British Standards Institution (BSI), London, UK, Dec. 2023. Available: https://knowledge.bsigroup.com/products/hydraulic-fluid-power-general-rules-and-safety-requirements-for-systems-and-their-components

[4] Parker Hannifin Corporation, *Industrial Hydraulic Technology Handbook*. Cleveland, OH: Parker Hannifin, 2015. Available: https://www.parker.com/content/dam/Parker-com/Literature/Hydraulics-Group-US/Industrial_Hydraulics_SG-HY01-1001.pdf